



**HAL**  
open science

## Extension of the MIMO Precoder based on the Minimum Euclidean Distance: a cross-form matrix

Baptiste Vrigneau, Jonathan Letessier, Phillippe Rostaing, Ludovic Collin,  
Gilles Burel

► **To cite this version:**

Baptiste Vrigneau, Jonathan Letessier, Phillippe Rostaing, Ludovic Collin, Gilles Burel. Extension of the MIMO Precoder based on the Minimum Euclidean Distance: a cross-form matrix. IEEE Journal on Selected Areas in Communications, 2008, 2 (2), pp.135-146. 10.1109/JSTSP.2008.922476. hal-00395147

**HAL Id: hal-00395147**

**<https://hal.univ-brest.fr/hal-00395147v1>**

Submitted on 11 May 2023

**HAL** is a multi-disciplinary open access archive for the deposit and dissemination of scientific research documents, whether they are published or not. The documents may come from teaching and research institutions in France or abroad, or from public or private research centers.

L'archive ouverte pluridisciplinaire **HAL**, est destinée au dépôt et à la diffusion de documents scientifiques de niveau recherche, publiés ou non, émanant des établissements d'enseignement et de recherche français ou étrangers, des laboratoires publics ou privés.

Copyright

# Extension of the MIMO Precoder based on the Minimum Euclidean Distance: a cross-form matrix

Baptiste Vrigneau, Jonathan Letessier, Philippe Rostaing, Ludovic Collin and Gilles Burel, *IEEE member*

**Abstract**—Under full channel state information at the transmitter side (Tx-CSI), MIMO precoders can be designed by the optimization of many pertinent criteria, like, for example, the maximizing post-processing signal-to-noise ratio (max-SNR or beamforming solution), or the minimizing weighted mean square error between transmit and receive vector-symbols (W-MMSE solution). These solutions decouple the MIMO channel into  $b$  parallel independent datastreams. This diagonal structure reduces the complexity of the maximum likelihood (ML) decisions but the diversity order of these schemes is limited. Recently, we proposed a precoder, max- $d_{\min}$  solution, which optimizes the exact expression of the minimum Euclidean distance and leads to a non diagonal structure allowing to achieve maximum diversity order. However, the result is available only for two transmit datastreams ( $b = 2$ ) and BPSK and QPSK modulations. In this paper, we propose a heuristic method to deal with the case  $b > 2$ , which provides a suboptimal, but good solution to this general problem. The new precoder, Equal- $d_{\min}$  (E- $d_{\min}$ ), is based on a non diagonal cross-form structure. It significantly enhances the transmit diversity in the eigen-subchannels. We demonstrate that the achieved diversity order is greater than that of precoders with diagonal structure for the same number of datastreams despite a trade-off between rate and diversity. This design can also ensure quality of service (QoS) by using an adapted power allocation strategy. Performance comparisons show the BER improvement for MIMO and MIMO-OFDM systems.

**Index Terms**—MIMO, max- $d_{\min}$  precoder, beamforming, Tx-CSI, diversity order trade-off, OFDM, QoS.

## I. INTRODUCTION

**T**HE multiple-input multiple-output (MIMO) systems used in a rich scattering environment for wireless communications improve significantly the reliability or the data rate of transmissions in comparison with single-input single-output (SISO) systems [1], [2]. MIMO techniques are adopted in wireless standards, such as 802.11n, for high data rate services. Various transmission strategies are adopted to improve the link reliability or/and spectral efficiency of very high data rate communication for wireless transmissions. The MIMO techniques can be classified into two categories often referred to as open-loop and closed-loop MIMO systems.

Open-loop systems do not require any channel state information (CSI) at the transmitter side. The link reliability is improved thanks to transmit diversity which is generally ensured by space-time techniques[3], [4], [5]. The most well known open-loop technique is the Alamouti Orthogonal Space-Time Bloc Code (OSTBC) for two transmit antenna with

a symbol rate 1. However, the use of space-time diversity techniques for transmission over fading channels reduce the data symbol rate in comparison with spatial multiplexing (SM) system.

Alternatively, closed loop transmit diversity is used in wireless MIMO systems, wherein each antenna can transmit an independent datastream into the wireless channels whereby the overall transmission rate is increased. Closed-loop MIMO methods allow to greatly improve the performance of MIMO communications if full channel knowledge is known at the transmitter (Tx-CSI). The Tx-CSI can be achieved by the transmitter with two methods: if the channel is slowly fading, the receiver estimates the channel and these data are fed back through a feedback link (typically in a Frequency Division Duplexing (FDD) mode), or the channel is considered as reciprocal, and the transmitter estimates the channel matrix thanks to a pilot signal issued from the receiver in a Time Division Duplexing (TDD) mode. In wireless MIMO orthogonal frequency division multiplexing (OFDM) standards, such as Wi-Fi (802.11n) or Wi-Max (802.16e), the singularvalues decomposition (SVD) type of beamforming technique is proposed. Using SVD, a MIMO channel can be decomposed into several independent subchannels for data transmission for each subcarrier [6].

The use of full Tx-CSI allows to design linear precoder and decoder by optimizing pertinent criteria such as, for example, maximizing the received signal-to-noise ratio[7], [8] (also referred to as single beamforming solution for one transmit symbol or multiple beamforming for more than one independent transmit symbol), minimizing the mean square error (MMSE)[9], [10], maximizing the capacity (Water-Filling solution). These solutions decouple the MIMO channel into independent and parallel datastreams. They are all based on SVD techniques by performing a power allocation strategy into the MIMO eigen-subchannels. The optimized precoding matrix is diagonal in the eigen-channel representation and belongs to an important subset of linear precoders named *diagonal precoders*. In addition, a suboptimal MBER solution (minimum bit-error-rate (BER): average BER over the substreams) can be derived directly from the diagonalized channel [11].

On the other hand, a unified framework is proposed in [6], [12] to design joint transmit-receive matrices based on the minimization of some arbitrary objective functions of the MSEs of all channel substreams. The authors in [6] obtain that for Schur-concave functions the channel matrix is fully diagonalized and for Schur-convex functions the channel matrix is diagonalized up to a specific rotation matrix, which

The authors are with LEST-UMR CNRS 6165, 6 Av. Le Gorgeu, CS 93837, 29238 Brest Cedex 3, France (e-mail: baptiste.vrigneau@univ-brest.fr; jonathan.letessier@univ-brest.fr; philippe.rostaing@univ-brest.fr; ludovic.collin@univ-brest.fr; gilles.burel@univ-brest.fr)

leads to a non diagonal structure. An interesting result is that the solutions which depend directly on the BER like, for example, the minimization of the maximum BER of the substreams, the maximization of the minimum SNR of the substreams (performance in term of BER is dominated by the substream with lowest SNR) or the minimization of the average BER over the substreams, are derived from optimizing Schur-convex functions of the MSE of all channel substreams. Thus, the resulting solutions have the non-diagonal structure: the power allocation into the MIMO eigen-subchannels is still performed but beforehand, a channel-independent specific rotation matrix mixes the transmit symbols[6].

An alternative solution leading to a non-diagonal structure is given in [13] by maximizing the minimum distance ( $\max-d_{\min}$ ) of the symbols at the receiver side. According to performance (BER enhancement) [14], [15], this  $\max-d_{\min}$  precoder is a promising solution compared to diagonal precoders. Unfortunately, the  $\max-d_{\min}$  result is available for two independent transmit symbols along with Binary Phase Shift Keying (BPSK) and 4-QAM (Quadrature Amplitude Modulation). The restriction to BPSK and 4-QAM results from the difficulty of the  $d_{\min}$  optimization and the general problem is still open [12, p.512]. Indeed, the exact expression of the minimum distance, which depends on the channel matrix, the modulation and the number of datastreams, is kept in the calculus.

This paper proposes a heuristic solution of this difficult optimization based on the  $\max-d_{\min}$  solution. The solution reveals two sources of suboptimality: *i*) the structure is based on 2x2 subsystems and *ii*) the modulation is limited to 4-QAM. However, this new linear precoder increases the number of transmit symbols and offers a compromise between the exact optimization of  $d_{\min}$  and the complexity, which is exponentially related to the number of datastreams. On the other hand, a trade-off between the diversity order and the data rate has been evidenced [16]. Thus, for a given number of antennas, any increase of the number of transmit symbols lowers the diversity order [17]. However, the precoder proposed here achieves a higher diversity order than diagonal precoders for the same number of transmit symbols. This characteristic permits a significant improvement of the transmission BER with the same transmit power. In order to compare the BER performance with the beamforming proposed by the 802.11n standard, this extended  $\max-d_{\min}$  precoder is applied to MIMO-OFDM system.

This paper is structured as follows: in section II, the system model is described with the matrix notation and the eigenmode representation. The  $\max-d_{\min}$  solution for two transmit symbols is presented in Section III. Section IV is devoted to the new precoder, which extends the  $\max-d_{\min}$  to an even number of symbols; an application of this solution to MIMO-OFDM systems is also proposed. Section V deals with the diversity order and compares it to diagonal precoders. In Section VI, the performances of  $\max-d_{\min}$  extension are highlighted through BER simulations in different case-studies. Our conclusions are drawn in Section VII.

## II. CHANNEL MODEL AND EIGENMODE REPRESENTATION

Let us consider a MIMO system with  $n_T$  transmit and  $n_R$  receive antennas, *i.e.* a  $(n_T, n_R)$  MIMO system, and assume a quasi-static flat-fading channel model, the received signal is therefore:

$$\mathbf{y} = \mathbf{G}\mathbf{H}\mathbf{F}\mathbf{s} + \mathbf{G}\mathbf{n} \quad (1)$$

where  $\mathbf{y}$  is the  $b \times 1$  received symbol vector,  $\mathbf{H}$  is the  $n_R \times n_T$  channel matrix,  $\mathbf{F}$  is the  $n_T \times b$  linear precoder matrix,  $\mathbf{G}$  is the  $b \times n_R$  linear decoder matrix,  $\mathbf{s}$  is the  $b \times 1$  transmitted symbol vector, and  $\mathbf{n}$  is the zero-mean  $n_R \times 1$  additive noise vector. Let us assume that  $b \leq \text{rank}(\mathbf{H}) \leq \min(n_T, n_R)$  and<sup>1</sup>

$$E[\mathbf{s}\mathbf{s}^*] = \mathbf{I}_b, \quad E[\mathbf{s}\mathbf{n}^*] = \mathbf{0} \quad \text{and} \quad E[\mathbf{n}\mathbf{n}^*] = \mathbf{R} \quad (2)$$

with  $\mathbf{R}$  the noise covariance matrix.

In addition, the average transmit power is limited to  $E_T$ :

$$\|\mathbf{F}\|_F^2 = E_T. \quad (3)$$

It is further assume that the transmitter and the receiver have perfect CSI. The main objective in this section is to obtain a diagonalized channel matrix and a whitened noise respectively called the virtual channel and the virtual noise: this operation is denoted virtual transformation [13]. By using the following decompositions  $\mathbf{F} = \mathbf{F}_v\mathbf{F}_d$  and  $\mathbf{G} = \mathbf{G}_d\mathbf{G}_v$ , the input-output relation (1) can be re-expressed as:

$$\mathbf{y} = \mathbf{G}_d\mathbf{H}_v\mathbf{F}_d\mathbf{s} + \mathbf{G}_d\mathbf{n}_v \quad (4)$$

where  $\mathbf{H}_v = \mathbf{G}_v\mathbf{H}\mathbf{F}_v$  is the eigen-channel matrix,  $\mathbf{n}_v = \mathbf{G}_v\mathbf{n}$  is the transformed additive noise vector with the covariance matrix  $\mathbf{R}_{n_v} = E[\mathbf{n}_v\mathbf{n}_v^*] = \mathbf{I}_b$ , the unitary matrices  $\mathbf{G}_v$  and  $\mathbf{F}_v$  are chosen so as to whiten the noise, diagonalize the channel and reduce dimension to  $b$ . This procedure based on the singularvalue decomposition (SVD) of  $\mathbf{H}$  is frequently used for MIMO systems, and the eigen-channel matrix is diagonal and denoted as:

$$\mathbf{H}_v = \text{diag}(\sigma_1, \sigma_2, \dots, \sigma_b). \quad (5)$$

The power constraint (3) is equivalent to:

$$\|\mathbf{F}_d\|_F^2 = E_T. \quad (6)$$

Some precoders are defined by a diagonal matrix  $\mathbf{F}_d = \text{diag}(f_1, f_2, \dots, f_b)$  and belong to the diagonal precoder group (see Fig. 1). There are solutions of criteria optimizations such as maximizing the channel capacity [2], minimizing the mean square error (MMSE)[9], [10], minimizing the BER (MBER) [11], maximizing the post-processing SNR [7], [8] (also often referred to as the single beamforming for one transmit symbol or the multiple beamforming by sending more than one symbol simultaneously [18]), or maximizing the minimum eigenvalue of the SNR-like matrix  $SNR(\mathbf{F}_D) = (\mathbf{H}_v\mathbf{F}_d)^2$  [10] (this precoder is equivalent to the Equal Error or EE that achieves the same BER on each datastream [9]). These

<sup>1</sup> $E[\cdot]$  denotes the expectation operator,  $(\cdot)^*$  the transpose conjugate,  $\mathbf{I}_n$  the  $(n \times n)$  identity matrix,  $\mathcal{N}_c(0, 1)$  the complex-normal zero-mean and unit-variance distribution,  $\|\mathbf{x}\|$  the Euclidean vector norm of the vector  $\mathbf{x}$ ,  $\text{trace}(\mathbf{A}\mathbf{A}^*) = \|\mathbf{A}\|_F^2$  the square of the Frobenius norm of the matrix  $\mathbf{A}$ ,  $\mathcal{C}$  the constellation alphabet and  $M = \text{card}(\mathcal{C})$  the constellation size, and  $\text{diag}(\cdot)$  the diagonal matrix.

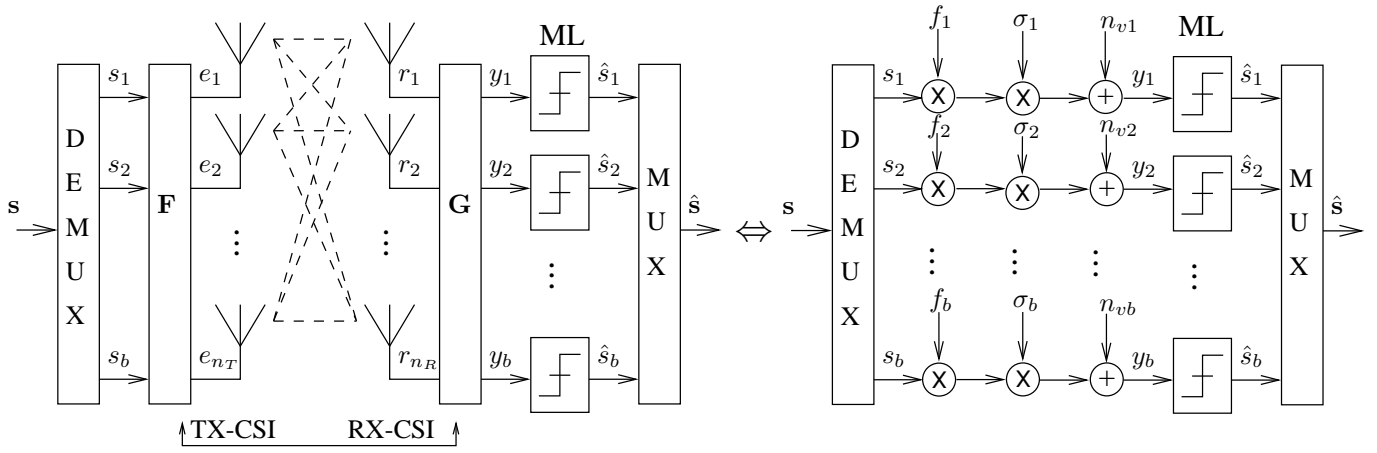


Fig. 1. MIMO block diagram with linear precoder and decoder for the diagonal solutions: the optimization of  $(\mathbf{F}, \mathbf{G})$  leads to a diagonalized channel with eigenmode power allocation and independent ML decisions with a complexity of  $b \times M$ .

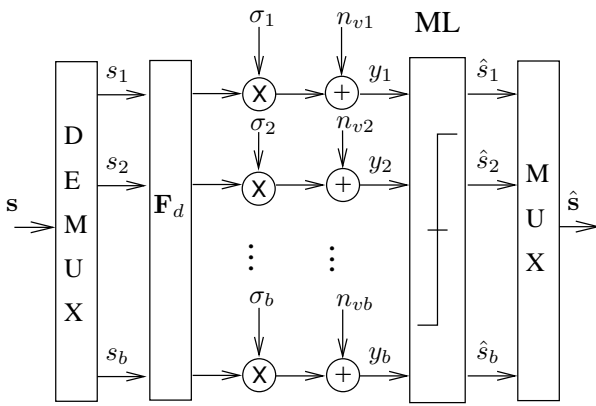


Fig. 2. MIMO block diagram of a non-diagonal general  $\max\text{-}d_{\min}$  precoder: the ML decision searches over all candidate transmitted symbol vectors and gives a complexity of  $M^b$  ( $b \times M$  for a diagonal precoder).

solution decouple the MIMO channel into  $b$  parallel independent datastreams as shown by the block diagram in Fig. 1. The MIMO system is equivalent to parallel SISO transmissions, and the ML decisions are simplified with only  $b \times M$  distances to be compared. Consequently, the diagonal precoders (*i.e.*  $\mathbf{F}_d$  is a diagonal matrix) have a low ML complexity, but do not use transmit diversity in the eigen-subchannels and do not achieve the maximum diversity order [17].

However, the particular case of the single beamforming solution or  $\max\text{-SNR}$  corresponding to the case  $b = 1$  achieves the maximum diversity order [19].

In the next section, we point out the key results of a non-diagonal precoder proposed in [13] by optimizing the minimum distance for two datastreams ( $b = 2$ ) which will be necessary for the extension to an arbitrary even number of datastreams ( $b \geq 4$ ).

### III. TWO-DIMENSIONAL OPTIMIZED $d_{\min}$ PRECODER: 2D- $\max\text{-}d_{\min}$ SOLUTION

The minimum Euclidean distance between signal points at the receiver side affects the system performances, especially with the ML detector [20]. From this well-known report, the

authors in [13] designed a new precoder based on the maximization of the minimum Euclidean distance. The minimum Euclidean distance  $d_{\min}$  is defined by:

$$d_{\min}(\mathbf{F}_d) = \min_{(\mathbf{s}_k, \mathbf{s}_l) \in \mathcal{C}^b, \mathbf{s}_k \neq \mathbf{s}_l} \|\mathbf{H}_v \mathbf{F}_d (\mathbf{s}_k - \mathbf{s}_l)\| \quad (7)$$

where  $\mathbf{s}_k$  and  $\mathbf{s}_l$  are two symbols vectors whose entries are elements of  $\mathcal{C}$ . Then, the  $\max\text{-}d_{\min}$  precoder is the solution of:

$$\mathbf{F}_d^{d_{\min}} = \arg \max_{\mathbf{F}_d} d_{\min}(\mathbf{F}_d) \quad (8)$$

under the power constraint  $\|\mathbf{F}_d\|_F^2 = E_T$ .

The comparison of the equivalent virtual scheme for a diagonal precoder (Fig. 1) and for a non-diagonal  $\max\text{-}d_{\min}$  one (Fig. 2) shows that the main difference is the ML complexity:  $M^b$  distances against  $b \times M$ .

The solution of (8) is difficult because the exact expression of  $d_{\min}$  is considered and depends on both the constellation size and the eigen-subchannels. A very exploitable solution of (8) was given in [13] for two independent datastreams,  $b = 2$  and a 4-QAM. In this case, the 2-dimensional eigen-channel matrix  $\mathbf{H}_v = \text{diag}(\sigma_1, \sigma_2)$  is rewritten for simplification purpose as:

$$\begin{cases} \sigma_1 = \rho \cos \gamma \\ \sigma_2 = \rho \sin \gamma \end{cases} \Leftrightarrow \begin{cases} \gamma = \arctan \frac{\sigma_2}{\sigma_1} \\ \rho = \sqrt{\sigma_1^2 + \sigma_2^2} \end{cases} \quad (9)$$

where  $\rho$  is a positive real parameter related to the eigen-channel gain, and  $\gamma$  is an angle linked to the singularvalues ratio and meeting  $\sigma_1 \geq \sigma_2 > 0$ , *i.e.*  $\pi/4 \geq \gamma > 0$ . It is worth noting that  $\mathbf{H}_v$  is totally defined by  $\rho$  and  $\gamma$ . Moreover, a small  $\gamma$  means that the first eigen-subchannel is privileged ( $\sigma_1 \gg \sigma_2$ ), whereas a value close to  $\pi/4$  indicates two close eigen-subchannels ( $\sigma_1 \simeq \sigma_2$ ). Then, the solution given in [13]

is SNR-independent and simply depends on the value of  $\gamma$ :

$$\mathbf{F}_d^{d_{\min}} = \mathbf{F}_{r1} = \begin{cases} \text{if } 0 \leq \gamma \leq \gamma_0, \\ \sqrt{E_T} \begin{pmatrix} \sqrt{\frac{3+\sqrt{3}}{6}} & \sqrt{\frac{3-\sqrt{3}}{6}} e^{i\frac{\pi}{12}} \\ 0 & 0 \end{pmatrix} \end{cases} \quad (10)$$

$$\mathbf{F}_d^{d_{\min}} = \mathbf{F}_{octa} = \begin{cases} \text{if } \gamma_0 \leq \gamma \leq \pi/4, \\ \sqrt{\frac{E_T}{2}} \begin{pmatrix} \cos \psi & 0 \\ 0 & \sin \psi \end{pmatrix} \begin{pmatrix} 1 & e^{i\frac{\pi}{4}} \\ -1 & e^{i\frac{\pi}{4}} \end{pmatrix} \end{cases} \quad (11)$$

$$\text{where } \begin{cases} \psi = \arctan \frac{\sqrt{2}-1}{\cos \gamma} \\ \gamma_0 = \arctan \sqrt{\frac{3\sqrt{3}-2\sqrt{6}+2\sqrt{2}-3}{3\sqrt{3}-2\sqrt{6}+1}} \simeq 17.28^\circ. \end{cases} \quad (12)$$

The term  $\psi$  is related to the eigenmode power allocation alike the diagonal precoders, and the constant threshold  $\gamma_0$  permits the precoder to use one (10) or two (11) eigen-subchannels. The  $\gamma_0$  value is computed by considering that the two precoding forms provide the same  $d_{\min}$ . Equations (10), (11) and (12) can be directly computed to design the 2D-max- $d_{\min}$  precoder for a given eigen-channel matrix or a value of  $\gamma$ . The optimized 2D minimum distance, noted  $\delta(\rho, \gamma)$ , depends on  $\rho$  and  $\gamma$  and is expressed as [13]:

$$d_{\min}(\mathbf{F}_d^{d_{\min}}) = \delta(\rho, \gamma) = \begin{cases} \sqrt{E_T} \rho \sqrt{1 - \frac{1}{\sqrt{3}} \cos \gamma} & \text{if } 0 < \gamma \leq \gamma_0 \\ \sqrt{E_T} \rho \sqrt{\frac{(4-2\sqrt{2}) \cos^2 \gamma \sin^2 \gamma}{1+(2-2\sqrt{2}) \cos^2 \gamma}} & \text{otherwise.} \end{cases} \quad (13)$$

In spite of the increase in ML complexity, the 2D-max- $d_{\min}$  precoder exploits the spatial diversity better than the diagonal precoders for two datastreams as shown in [15], [14]. Indeed, this promising precoder achieves a significant SNR gain when  $n_T$  and  $n_R$  are increased but is limited for  $b = 2$ . The following section introduce an extension of the max- $d_{\min}$  for  $b > 2$ .

#### IV. EXTENSION OF THE max- $d_{\min}$ PRECODER

##### A. Principle: decomposition into 2D-max- $d_{\min}$ subsystems

Let us consider an even number of data streams,  $b \geq 4$ , for large MIMO systems ( $\min(n_T, n_R) \geq 4$ ). The optimization (8) for  $b > 2$  being difficult, it leads us to propose a compromise between the  $d_{\min}$  optimization and the complexity of the solution. The main idea is to decompose the  $(b \times b)$  eigen-channel matrix into  $(2 \times 2)$  eigen-channel matrices, which are  $d_{\min}$ -optimized for two datastreams (see Fig. 3). Then, the extension is split into four steps:

- 1) A virtual transformation of  $\mathbf{H}$  with  $b > 2$  gives a diagonal matrix  $\mathbf{H}_v$  (5) with the  $b$  ordered singularvalues (SV).
- 2) The association of  $b/2$  couples of singularvalues leads to  $b/2$  2D-virtual systems, denoted subsystem  $\#i$ , for  $i = 1, \dots, b/2$  as it is illustrated in Fig. 3. Note that, in the figure, the best singularvalues association is given and it will be shown further in the subsection IV-C.
- 3) The application of the optimal 2D-max- $d_{\min}$  solution on the subsystem  $\#i$  determines the matrix  $\tilde{\mathbf{F}}_{di}$  with

the power constraint  $\|\tilde{\mathbf{F}}_{di}\|_F^2 = 1$ , for  $i = 1, \dots, b/2$ . Then, the subsystem  $\#i$  gives the minimum distance:

$$\delta_i = d_{\min}(\tilde{\mathbf{F}}_{di}^{d_{\min}}) \quad \text{given by (13) with } E_T = 1. \quad (14)$$

- 4) At last, the power is allocated by the coefficient  $\Upsilon_i$ , to the subsystem  $\#i$ , for  $i = 1, \dots, b/2$ , under the power constraint  $\sum_i \Upsilon_i^2 = E_T$ , in order to maximize the minimum distance:

$$\Delta = \min_i \Upsilon_i \delta_i. \quad (15)$$

This proposed scheme limits the complexity of the ML decisions: the number of distances to be compared is  $b/2 \times M^2$ . This complexity is still higher than that of the diagonal precoders ( $b \times M$ ), but it is not exponential ( $M^b$  for a general non-diagonal solution).

As Steps 1 and 3 are already known, the better singularvalues association (step 2) and a criterion for the power allocation (step 4) have still to be determined. However, the proposed solution of step 4 is independent from step 2, and the optimization problem can be decoupled.

##### B. Power allocation $\Upsilon$ : Equal $d_{\min}$ precoder (E- $d_{\min}$ )

The criterion of the power allocation is the maximization of the minimum distance  $\Delta$ . Thus,  $\Upsilon$  is the solution of:

$$\max_{\Upsilon} \min_i \Upsilon_i \delta_i \quad \text{and} \quad \sum_{k=1}^{b/2} \Upsilon_k^2 = E_T \quad (16)$$

with  $\Upsilon = [\Upsilon_1, \Upsilon_2, \dots, \Upsilon_{b/2}]$ . The optimized solution of the power allocation,  $\Upsilon$ , consists in equalizing the distances (*i.e.*  $d_{\min} = \Upsilon_i \delta_i$  for all  $i$ ). Thus, by using the power constraint (16), we obtain

$$E_T = \sum_{k=1}^{b/2} \frac{d_{\min}^2}{\delta_k^2} = \Upsilon_i^2 \delta_i^2 \sum_{k=1}^{b/2} \frac{1}{\delta_k^2}$$

and the the power allocation is then given by

$$\Upsilon_i^2 = E_T \left( \delta_i^2 \sum_{k=1}^{b/2} \frac{1}{\delta_k^2} \right)^{-1} \quad \text{for } i = 1, \dots, \frac{b}{2}. \quad (17)$$

This precoder is then denoted Equal  $d_{\min}$  or E- $d_{\min}$ . The power constraint can be verified:

$$\|\mathbf{F}_d\|_F^2 = \sum_{i=1}^{b/2} \Upsilon_i^2 \|\tilde{\mathbf{F}}_{di}\|_F^2 = \sum_{i=1}^{b/2} \Upsilon_i^2 = E_T. \quad (18)$$

By using (17), the optimized minimum distance  $d_{\min}$  is:

$$d_{\min}^2 = \Upsilon_i^2 \delta_i^2 = E_T \left( \sum_{k=1}^{b/2} \frac{1}{\delta_k^2} \right)^{-1}. \quad (19)$$

The minimum distance depends on the inverse of the square minimum distance of each subsystem.



This form highlights a diagonal precoder (the diagonal elements) where each element is associated with a new one (the antidiagonal elements) in order to enhance the symbol transmission: with respect to diagonal precoders, this precoder introduces transmit diversity in the eigen-subchannels.

### E. Extension to OFDM MIMO system

A beamforming precoder adapted to the MIMO channel at each subcarrier was proposed in the ongoing standardization IEEE 802.11n [21]. With this system, each subcarrier has a quasi-static MIMO channel [22], and a global matrix can be defined as:

$$\mathbf{H} = \begin{pmatrix} \mathbf{H}^{(1)} & 0 & \dots & 0 \\ 0 & \mathbf{H}^{(2)} & & \vdots \\ \vdots & & \ddots & 0 \\ 0 & 0 & \dots & \mathbf{H}^{(N)} \end{pmatrix} \quad (29)$$

where  $N$  is the number of subcarriers, and  $\mathbf{H}^{(i)}$  is the  $n_R \times n_T$  channel matrix for the  $i$ th subcarrier. As previously, the channel is diagonalized with the virtual transformation:

$$\mathbf{H}_v = \begin{pmatrix} \mathbf{H}_v^{(1)} & 0 & \dots & 0 \\ 0 & \mathbf{H}_v^{(2)} & & \vdots \\ \vdots & & \ddots & 0 \\ 0 & 0 & \dots & \mathbf{H}_v^{(N)} \end{pmatrix} \quad (30)$$

where  $\mathbf{H}_v^{(i)}$  is the  $b \times b$  virtual channel of  $\mathbf{H}^{(i)}$  and is diagonal,  $\mathbf{H}_v^{(i)} = \text{diag}(\sigma_1^{(i)}, \dots, \sigma_b^{(i)})$ . In the 802.11n standard, only the first eigenvalue is kept by the beamforming precoder, *i.e.*  $b = 1$ . However, the other values can offer transmit diversity exploited by the E- $d_{\min}$  precoder. The global virtual matrix,  $\mathbf{H}_v$ , is reorganized to get a diagonal matrix with ordered elements:

$$\tilde{\mathbf{H}}_v = \text{diag}(\text{sort}(\sigma_1^{(1)}, \dots, \sigma_b^{(1)}, \dots, \sigma_1^{(N)}, \dots, \sigma_b^{(N)})) \quad (31)$$

where the values are ranked in descending order by the operator *sort*. The final operation consists in applying the E- $d_{\min}$  solution to this new virtual matrix  $\tilde{\mathbf{H}}_v$ .

## V. E- $d_{\min}$ DIVERSITY ORDER

### A. Proven evidence of diversity order

To provide theoretical evidence of E- $d_{\min}$  diversity order, let us proceed as done in [19] for the max-SNR: the system under consideration is a  $(n_T, n_R)$  MIMO system with a single frequency carrier (no OFDM) associated to the E- $d_{\min}$  solution. In addition, let us assume that the channel is uncorrelated Rayleigh fading and that the noise is an additive white gaussian noise (*i.e.*  $\mathbf{R}_n = \sigma_n \mathbf{I}_{n_R}$ ). On these assumptions, the eigen-subchannel  $\sigma_i$  is equal to  $\sqrt{\lambda_i}/\sigma_n$  where  $\lambda_i$  are the eigenvalues of  $\mathbf{H}\mathbf{H}^*$  for  $i = 1, \dots, b$ . At first, let us consider a subsystem  $\#i$  with the subprecoder,  $\tilde{\mathbf{F}}_{d_i}$ , and the power allocation  $\Upsilon_i^2$  (see Fig.3). The symbol error probability (SEP) of each subsystem can be tightly approximated by [23]:

$$\text{SEP}_i \simeq \frac{\bar{N}_e}{2} \text{erfc} \left( \sqrt{\Upsilon_i^2 \tilde{d}_i^2 / (4\sigma_n^2)} \right) \quad (32)$$

where  $\bar{N}_e$  is a constant related to the average number of the nearest neighbors and  $\tilde{d}_i$  given in (25). At high SNR, the Chernoff bound can be used to approximate the erfc function ( $\text{erfc}(x) \simeq e^{-x^2}$ ):

$$\text{SEP}_i \simeq \frac{\bar{N}_e}{2} e^{-\Upsilon_i^2 \tilde{d}_i^2 / (4\sigma_n^2)}. \quad (33)$$

One should note that, with E- $d_{\min}$  solution, the term  $\Upsilon_i^2 \tilde{d}_i^2 = d_{\min}^2$  is the same whatever  $i$  ( $i = 1, \dots, b/2$ ) and, thus, the demonstration of the diversity order is the same for all subsystems.

*Lemma 2:* The minimum distance (19) computed with the optimized SV association (26) can be upper- and lower-bounded as:

$$E_T \frac{2}{b} \xi \lambda_{b/2} \leq d_{\min}^2 \leq E_T \lambda_{b/2} \quad (34)$$

where  $\xi = 1 - \frac{1}{\sqrt{3}}$ .

*Proof:* see appendix II. ■

By using equations (33) and (34), SEP can be upper- and lower-bounded as:

$$\frac{\bar{N}_e}{2} e^{-\frac{\text{SNR} \lambda_{b/2}}{4}} \leq \text{SEP}_i \leq \frac{\bar{N}_e}{2} e^{-\frac{\text{SNR} \frac{2}{b} \xi \lambda_{b/2}}{4}} \quad (35)$$

where  $\text{SNR} = E_T/\sigma_n^2$ . As the term,  $\lambda_{b/2}$ , is a random variable, SEP has to be averaged:

$$\overline{\text{SEP}}_i = E[\text{SEP}_i] \quad (36)$$

In [18], the averaged result was given over the probability density function (pdf) of  $\lambda_i$ :

$$\int_0^\infty e^{-\beta \lambda_i} f_{\lambda_i}(\lambda_i) d\lambda_i \simeq \epsilon (\beta/m)^{-(n_T-i+1)(n_R-i+1)} \quad (37)$$

where  $m = \min(n_T, n_R)$  and  $\epsilon$  is a constant. Thus applying (37) to (35) leads to:

$$\frac{\bar{N}_e}{2} \epsilon (\text{SNR}/(4m))^{-(n_T-b/2+1)(n_R-b/2+1)} \leq \overline{\text{SEP}}_i \leq \frac{\bar{N}_e}{2} \epsilon (\xi \text{SNR}/(2bm))^{-(n_T-b/2+1)(n_R-b/2+1)}. \quad (38)$$

It ensues that every subsystem and, consequently, the E- $d_{\min}$  precoder, has a diversity order equal to  $(n_T - b/2 + 1)(n_R - b/2 + 1)$ .

### B. Diversity Order Discussion

Further to the numerous studies devoted to the diversity order of precoders, the existence of a trade-off between diversity and multiplexing has become patent [16]. Thus, the max-SNR transmits one single symbol and achieves the maximum diversity  $n_T \times n_R$  [19]; when the diagonal precoders transmit  $b$  symbols, the diversity order achieved is equal to  $(n_T - b + 1)(n_R - b + 1)$  [18]. In [14], we already mentioned that, despite the transmission of two symbols by the 2D-max- $d_{\min}$  precoder, the maximum diversity order  $n_T \times n_R$  is still achieved. The proposed extension E- $d_{\min}$  achieves  $(n_T - \frac{b}{2} + 1)(n_R - \frac{b}{2} + 1)$  for an even value  $b$ . This diversity order is not maximum but is higher than the one by the diagonal precoder because of the particular form of

$\mathbf{F}_d$ . The solution given in (27) is a cross-form matrix where a diagonal structure is associated to an antidiagonal one to create transmit diversity. However, this precoder can adapt the structure of the matrix  $\mathbf{F}_d$  according to the (2,2) eigenchannel matrices  $\tilde{\mathbf{H}}_{vi}$ . The elements  $f_1^{(i)}$  and  $f_2^{(i)}$  are never null unlike  $f_3^{(i)}$  and  $f_4^{(i)}$  which can be equal to zero depending on the numerical values of elements of  $\tilde{\mathbf{H}}_{vi}$  or more precisely the angles  $\gamma_i = \arctan(\sigma_{b-i+1}/\sigma_i)$  for  $i = 1, \dots, b/2$ . In the extreme case, the cross-form matrix can be changed into a V-form one ( $f_3^{(i)} = f_4^{(i)} = 0, \forall i$ ). The number of eigen-subchannels to be used is automatically set by the E- $d_{\min}$  precoder.

The table I permits one to compare the trade-off between the ML complexity and the diversity order. The SVD operation stands for all precoders. Note that the matrix  $\mathbf{F}_d$  in (27) can be directly computed via formulas (10)-(12), (13) and (17). The complexity of E- $d_{\min}$  is dominated by the ML search. The number of ML tests is given by  $M^2 b/2 = 8b$  ( $M = 4$  is fixed for the E- $d_{\min}$  solution). The ML complexity of the E- $d_{\min}$  grows linearly with  $b$ . Note that, with the same spectral efficiency, the diagonal precoders perform  $4b$  ML tests.

In conclusion, for a fixed number of datastreams, the diversity order with the E- $d_{\min}$  precoder is higher than the one by the diagonal precoders at the price of a reasonable increase in complexity (a number of ML tests twice larger).

## VI. SIMULATION RESULTS

The BER curves of the E- $d_{\min}$  precoder were assessed through 3 experiments respectively carried out to: *i*) evaluate its capabilities against those of diagonal precoders[10], [11] and the truly non-diagonal MBER precoder[6] *ii*) determine the impact of change in power allocation,  $\Upsilon$ , into QoS, and *iii*) compare the E- $d_{\min}$  extended to MIMO-OFDM systems with the 802.11n standard.

### A. First experiment: performance of the precoder E- $d_{\min}$

1) *BER enhancement*: Figure 4 illustrates the BER simulations for the E- $d_{\min}$  with  $b = 4$  4-QAM symbols. The precoder is compared to diagonal precoders (MBER [11] with  $b = 4$  symbols and EE[10] with  $b = 4$  or  $b = 2$  symbols) and also with the non-diagonal ARITH-MBER precoder[6] (truly MBER with  $b = 4$  or  $b = 2$  symbols). When a precoder transmits  $b = 4$  symbols, the associated modulation is 4-QAM, and when  $b = 2$ , a 16-QAM is used. Thus, each system has the same spectral efficiency which is equal to 8 bit/s/Hz and uses  $n_T = n_R = 4$  antennas.

The BERs were simulated for  $10^4$  random matrices  $\mathbf{H}$  ( $4 \times 4$ ) with i.i.d. entries according to complex normal distribution  $\mathcal{N}_c(0, 1)$ .

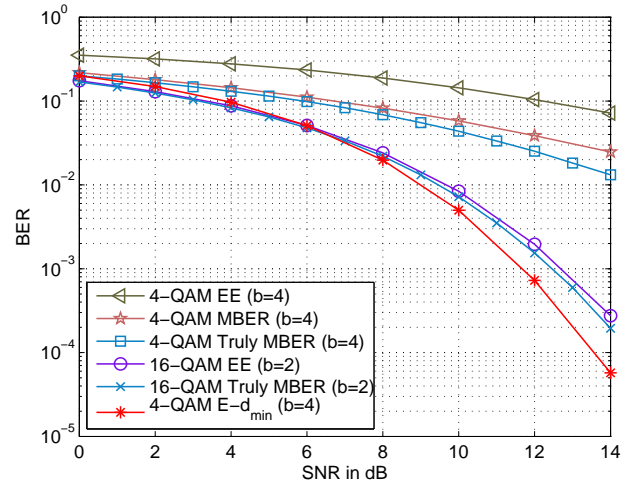


Fig. 4. Comparison of E- $d_{\min}$  ( $b = 4$ , 4-QAM symbols) with MBER ( $b = 4$ , 4-QAM), EE ( $b = 4$ , 4-QAM or  $b = 2$ , 16-QAM) and truly MBER ( $b = 4$ , 4-QAM or  $b = 2$ , 16-QAM) for a (4,4) MIMO system with 8 bit/s/Hz and uncorrelated Rayleigh fading channel.

For the same  $b = 4$  substreams and the same 4-QAM symbols, the truly MBER with a non diagonal structure enhances the BER compared to the diagonal precoders. However, the BER of the E- $d_{\min}$  precoder is largely improved thanks to the higher diversity order  $((n_T - b/2 + 1)(n_R - b/2 + 1) = 9$  against  $(n_T - b + 1)(n_R - b + 1) = 1$  for the diagonal one). The comparison of E- $d_{\min}$  with the truly MBER and the diagonal EE precoder with  $b = 2$  and 16-QAM shows<sup>2</sup> that the BER of the E- $d_{\min}$  precoder is significantly enhanced at high SNR. On the other hand, at SNR below 6 dB, the E- $d_{\min}$  is slightly less efficient than truly MBER and EE with  $b = 2$ . Note that, diagonal EE and MBER precoders with  $b = 2$  and 16-QAM give an equivalent BER performance and the diagonal MBER is not plotted for clarity.

This BER enhancement of E- $d_{\min}$  can be probably explained by the two following principal reasons:

- i*) the criterion based on the optimization of  $d_{\min}$  is particularly well suited for BER performance at high SNR regime,
- ii*) the  $d_{\min}$  optimization leads to the jointly estimation of the power allocation and the rotation matrix which depends on the eigen-subchannels (see (10) and (11)).

2) *Probability density function of  $\gamma_i$* : as the random variable  $\gamma_i$  is a key-parameter of the 2D-max- $d_{\min}$  solution, it sounded us worth studying the probability density function of this

<sup>2</sup>Note that for  $b = 2$ , the diagonal precoder increases the diversity order to  $(n_T - b + 1)(n_R - b + 1) = 9$  (same diversity order as E- $d_{\min}$ ).

TABLE I

TRADE-OFF BETWEEN THE ML COMPLEXITY AND THE DIVERSITY ORDER WITH  $\log_2(M)$  TRANSMIT BITS PER DATA-SUBSTREAM

Precoder	used subchannels	Number of ML tests	Diversity order
max-SNR	1	$M$	$n_T \times n_R$
Diagonal precoder	$b$	$bM$	$(n_T - b + 1)(n_R - b + 1)$
E- $d_{\min}$ ( $M = 4$ )	$b$	$\frac{b}{2}M^2$	$(n_T - b/2 + 1)(n_R - b/2 + 1)$

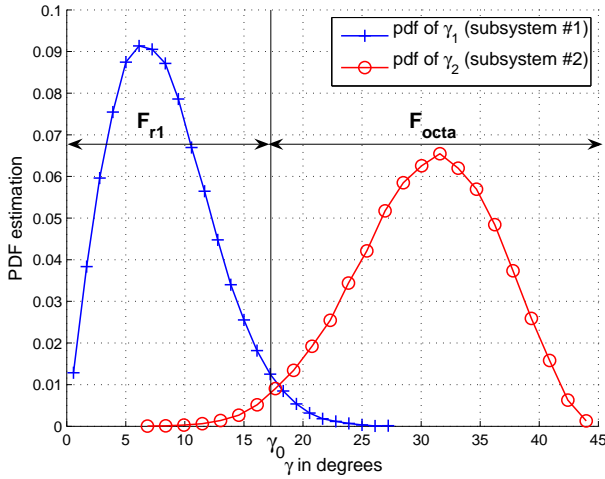


Fig. 5. Probability density functions of  $\gamma_1$  and  $\gamma_2$  angles for a (4,4) MIMO system with uncorrelated Rayleigh fading (estimation with  $10^5$  random channel matrices).

variable. Figure 5 plots the pdf of  $\gamma_1$  and  $\gamma_2$  for a (4,4) MIMO system with  $b=4$  and an uncorrelated Rayleigh fading channel. The angle,  $\gamma_1$ , corresponds to the couple  $(\sigma_1, \sigma_4)$ , and  $\gamma_2$  corresponds to  $(\sigma_2, \sigma_3)$ . Figure 5 highlights their different behaviors. Indeed,  $\gamma_1$  takes small values ( $E[\gamma_1] = 8^\circ \ll \gamma_0$ ): the subprecoder  $\tilde{\mathbf{F}}_{d1}$  statistically uses more often only  $\sigma_1$ . The probability is  $P[\tilde{\mathbf{F}}_{d1} = \mathbf{F}_{r1}] = P[\gamma_1 < \gamma_0] = 97\%$ . The second subprecoder  $\tilde{\mathbf{F}}_{d2}$  has a totally different strategy. Indeed,  $\sigma_2$  and  $\sigma_3$  are close ( $E[\gamma_2] = 30^\circ \gg \gamma_0$ ): the subprecoder statistically chooses to use the two eigen-subchannels. The probability is  $P[\tilde{\mathbf{F}}_{d2} = \mathbf{F}_{octa}] = 1 - P[\tilde{\mathbf{F}}_{d2} = \mathbf{F}_{r1}] = 1 - P[\gamma_2 < \gamma_0] = 98\%$ . It ensues that  $\tilde{\mathbf{F}}_{d1}$  is quasi equivalent to the max-SNR, whereas the second one,  $\tilde{\mathbf{F}}_{d2}$ , significantly exploits the diversity proposed by  $\sigma_2$  and  $\sigma_3$ . On the other hand, these probabilities depend on the number of antennas in use. Thanks to its ability to adapt the number of used eigen-subchannels, the  $E-d_{\min}$  can use all the singularvalues till the

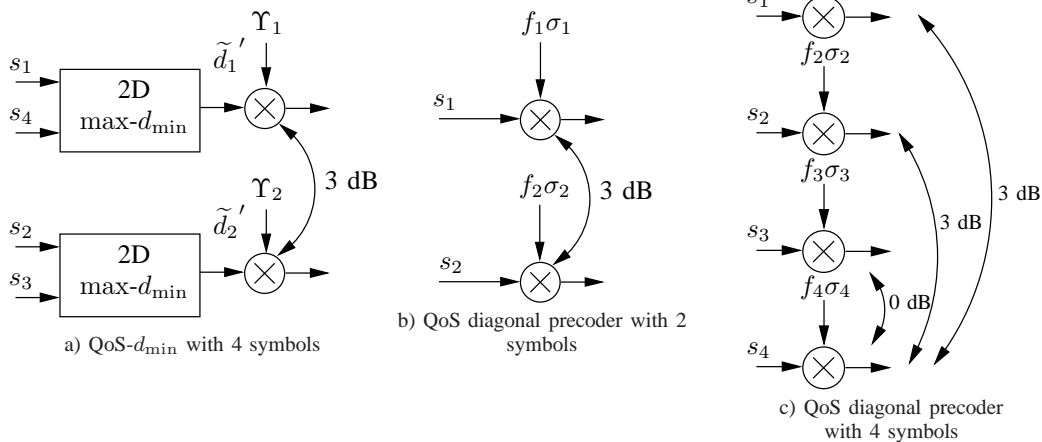


Fig. 6. Three possible 3dB-QoS synoptics: (a) QoS applied to the optimized minimum distance of two subsystems, (b) QoS applied to 2 eigen-subchannels and (c) QoS applied to 4 eigen-subchannels. Cases b) and c) correspond to the classical QoS diagonal precoder

TABLE II  
 PERCENTAGES OF THE NUMBER OF EIGEN-SUBCHANNEL USED BY THE  $E-d_{\min}$  PRECODER ( $b = 4$ ) FOR UNCORRELATED RAYLEIGH FADING CHANNEL

MIMO system	cross-form 4 eigen-subchannels: $(\sigma_1, \sigma_2, \sigma_3, \sigma_4)$	intermediate form 3 eigen-subchannels: $(\sigma_1, \sigma_2, \sigma_3)$	V-form 2 eigen-subchannels: $(\sigma_1, \sigma_2)$
(4,4)	3%	95%	2%
(6,6)	91%	9%	0%

$b/2$  highest one. Table II shows how the  $E-d_{\min}$  uses the SV for a (4,4) and (6,6) MIMO system: the cross-form is more often used for a (6,6) MIMO system.

B. Second experiment: power allocation  $\Upsilon$  based on QoS, the QoS- $d_{\min}$  precoder

The  $E-d_{\min}$  precoder presented above relies on a  $d_{\min}$ -maximizing power allocation (analog to the Error Equal precoder). This experiment was aimed at transforming the power strategy into a Quality of Service: for each subsystem, the  $\Upsilon_i d_i$ -to- $\Upsilon_{b/2} d_{b/2}$  ratio can be fixed in order to have about the same SNR gain in terms of BER performance between the subsystems  $\#i$  and  $\#b/2$ . For example, Fig. 6 shows three possible synoptics to ensure a 3dB-SNR gain. Let us consider  $b = 4$  4-QAM symbols  $s_1, s_2, s_3$  and  $s_4$  which are separated into two 2D-max- $d_{\min}$  subsystems. For each subsystem, the BER is simulated and should ensure a 3dB-SNR gain. This precoder is denoted QoS- $d_{\min}$ . However, in a QoS aim, the distances  $\tilde{d}_1, \dots, \tilde{d}_{b/2}$  needs to be reorganized in order to rank the  $\tilde{d}_i$ . The ranked distances are denoted  $\tilde{d}'_1 \geq \tilde{d}'_2 \geq \dots \tilde{d}'_{b/2}$ . The  $\Upsilon_i$  coefficients are determined so as to get a 3dB gain between  $\Upsilon_1 \tilde{d}'_1$  and  $\Upsilon_2 \tilde{d}'_2$  (Fig. 6.a) and the general solution is given by:

$$\Upsilon_i^2 = \frac{E_T \omega_i}{\tilde{d}_i^{r2} \sum_{k=1}^{b/2} \frac{\omega_k}{\tilde{d}_k^{r2}}} \quad \text{for } i = 1, \dots, b/2 \quad (39)$$

where  $\omega_1 \geq \omega_2 \geq \dots \geq \omega_{b/2}$  are the  $\tilde{d}_i^{r^2}$  ratios related to  $\tilde{d}_{b/2}^{r^2}$  ( $\omega_{b/2} = 1$ ). For the 3dB-QoS- $d_{\min}$  in Fig. 6.a, we fix  $w_1 = 2$  and  $w_2 = 1$ . This solution is compared to 2 diagonal precoders: the 3dB-QoS precoder with either  $b = 2$ , 16-QAM symbols (Fig. 6.b) or  $b = 4$ , 4-QAM symbols (Fig. 6.c). Figure 7 depicts the BER curves from simulations of the 3 precoders with an uncorrelated Rayleigh fading channel for a (4,4) MIMO system. For every precoder, it shows about 3dB gain between the first and second datastream BERs. The SNR gain for the QoS- $d_{\min}$  is slightly higher than 3dB. It also evidences that only two symbols have to be used by the QoS precoder to enhance the BER thanks to the diversity order. The diversity order is alike with the QoS- $d_{\min}$  and the QoS ( $b = 2$ , 16-QAM), but the former has a SNR gain of about 1.5 dB with respect to the latter. In conclusion, the QoS- $d_{\min}$  precoder can achieve quality of service while enhancing the transmission BER compared to the classical QoS diagonal precoder.

### C. Third experiment: application to the 802.11n OFDM standard

The current 802.11n specifications propose an optional narrowband beamforming approach for each subcarrier. Note that in the time division duplex mode, unlike frequency division duplex mode, closed loop operation is based on the reciprocity between uplink and downlink channels. This is a valid assumption as long as the delay between channels is small compared to the coherence time, as is usually the case in indoor environments. To compare the E- $d_{\min}$  precoder to the beamforming used in the 802.11n standard, BER simulations were run for a (2,2) MIMO system with 64 frequency subcarriers and  $b = 2$  symbols per subcarrier, *i.e.*  $64 \times 2 = 128$  transmit symbols in one OFDM symbol. The channel parameters are based on the European standard HIPERLAN/2 (ETSI BRAN HIPERLAN/2) for a wireless local area network [24] and correspond to a typical office environment under Non-Line of Sight (NLOS) conditions (150 ns average root mean squared delay spread and 1.1  $\mu$ s maximum delay). Moreover, the 2D-max- $d_{\min}$  precoder was applied to each subcarrier and simulated to evidence E- $d_{\min}$  enhancement. Figure 8 illustrates the simulations results with the 3 precoders and shows that the 2D-max- $d_{\min}$  and the max-SNR are appreciably equivalent for a (2,2) MIMO system as expected [15], [14]. These simulations clearly show a large BER improvement with the E- $d_{\min}$  compared to the max-SNR: it is of about 4 dB at a BER equal to  $10^{-3}$ . Thus, under the same conditions of Tx-CSI information and transmit power, the BER is significantly enhanced by the E- $d_{\min}$  precoder compared to the beamforming used in the 802.11n standard.

## VII. CONCLUSION

We introduced a new linear precoder for MIMO systems based on the maximization of the minimum Euclidean distance under an average total transmit power constraint. The principle of this precoder is to use the 2D-max- $d_{\min}$  optimal solution (available for BPSK and QPSK) as a base block and to associate it with a power allocation strategy. Despite this heuristic approach provides a suboptimal solution (the

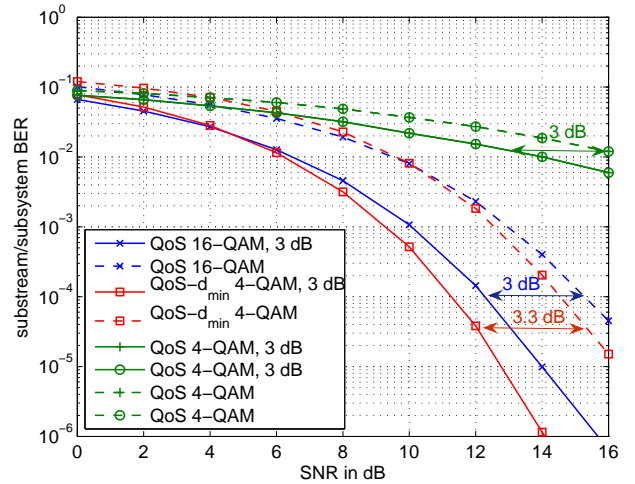


Fig. 7. BER simulations of the QoS- $d_{\min}$  compared to the diagonal QoS precoder ( $b = 2$ , 16-QAM or  $b = 4$ , 4-QAM) with a (4,4) MIMO uncorrelated Rayleigh fading channel.

optimal solution for the general case still being an open problem), it significantly improves previous results and is a good trade-off between the exact optimization and complexity. Moreover, if new optimal solution of 2D-max- $d_{\min}$  is found for others modulations, it will need no effort to be integrated to the E- $d_{\min}$ , due to the simple and regular structure of our precoder. It can transmit an even number of datastreams and, consequently, fully exploits large MIMO systems by increasing the data rate. This precoder has thus a diversity order higher than the diagonal solutions. Indeed, despite the trade-off between diversity and data rate, we demonstrated that the E- $d_{\min}$  precoder can transmit twice more symbols than a diagonal solution while keeping the same diversity order. Consequently, the BER of the E- $d_{\min}$  is significantly improved compared to either a diagonal solution with the same number of datastreams or a diagonal precoder with similar diversity order and spectral efficiency. In addition, the proposed solution is adaptable to other strategies such as quality of service where BER simulations showed an enhancement compared to the QoS diagonal precoder. At last, we extended the solution to MIMO-OFDM systems and compared it to the optimal beamforming proposed in the 802.11n standard. Under similar conditions of channel information and transmit power, the BER was significantly enhanced by the E- $d_{\min}$  precoder.

## APPENDIX I PROOF OF LEMMA 1

Before showing the Lemma, we establish three properties about the distances.

### A. Preliminaries: establishment of three properties

Let us prove the following three properties :

$$\delta(\sigma_a, \sigma) \geq \delta(\sigma_b, \sigma) \text{ if } \sigma \leq \sigma_b \leq \sigma_a \quad (40a)$$

$$\delta(\sigma, \sigma_a) \geq \delta(\sigma, \sigma_b) \text{ if } \sigma \geq \sigma_a \geq \sigma_b \quad (40b)$$

$$\delta(\sigma_a, \sigma_b) \geq \delta(\sigma_c, \sigma_d) \text{ if } \sigma_a > \sigma_b > \sigma_c > \sigma_d \quad (40c)$$

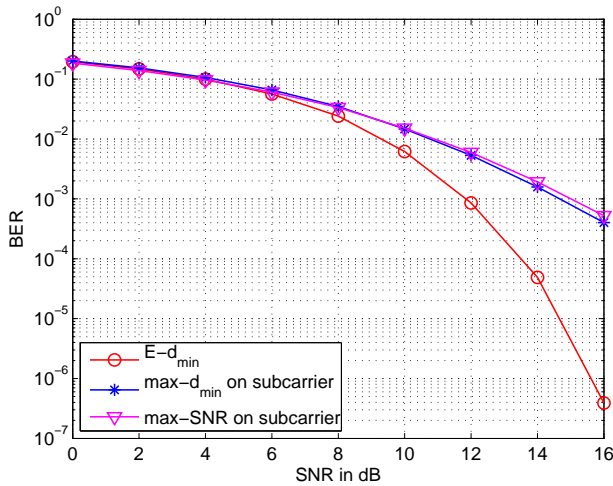


Fig. 8. BER simulation with the ETSI BRAN channel model for a (2,2) MIMO system and 64 subcarriers.

where  $\delta(\sigma_i, \sigma_j)$  is the optimized minimum distance associated with the SV couple  $(\sigma_i, \sigma_j)$  with  $\sigma_i \geq \sigma_j$  given by the 2D-max- $d_{\min}$  solution (i.e.  $\delta(\sigma_i, \sigma_j) \triangleq \delta(\rho, \gamma)$  with  $\sigma_i = \rho \cos \gamma$  and  $\sigma_j = \rho \sin \gamma$  in (13)).

*Proof of (40a):* we denote subsystem #a the subsystem using  $(\sigma_a, \sigma)$  and subsystem #b the subsystem using  $(\sigma_b, \sigma)$ . Three cases have to be studied when  $\sigma \leq \sigma_b \leq \sigma_a$ :

i) both subsystems use  $\mathbf{F}_{r1}$

The distances of the subsystems #a and #b are given by:  $\delta(\sigma_a, \sigma) = \sigma_a \sqrt{E_T(1 - 1/\sqrt{3})}$  and  $\delta(\sigma_b, \sigma) = \sigma_b \sqrt{E_T(1 - 1/\sqrt{3})}$ . Equation (40a) is then verified ( $\sigma_a > \sigma_b$ ).

ii) both subsystems use  $\mathbf{F}_{octa}$

The distance of the precoder  $\mathbf{F}_{octa}$  can be expressed as:

$$\delta(\sigma_1, \sigma_2) = \sqrt{E_T \frac{(4 - 2\sqrt{2})\sigma_2^2}{1 + (3 - 2\sqrt{2})\sigma_2^2/\sigma_1^2}}$$

For a fixed  $\sigma_2 = \sigma$ , this function is strictly increasing with  $\sigma_1$ . Consequently, we have  $\delta(\sigma_a, \sigma) > \delta(\sigma_b, \sigma)$ .

iii) subsystems #a and #b use  $\mathbf{F}_{r1}$  and  $\mathbf{F}_{octa}$ , respectively

First, note that  $\sigma_a > \sigma_b$  implies  $\gamma_a = \arctan(\sigma/\sigma_a) < \gamma_0 < \gamma_b = \arctan(\sigma/\sigma_b)$ , then from (10)-(12) subsystem #a uses  $\mathbf{F}_{r1}$  and subsystem #b uses  $\mathbf{F}_{octa}$ . The inverse case ( $\mathbf{F}_{octa}$  for subsystem #a and  $\mathbf{F}_{r1}$  for subsystem #b) is then not possible. The distance of the subsystem #a can be lower bounded

as:  $\delta(\sigma_a, \sigma) = \sigma_a \sqrt{E_T(1 - 1/\sqrt{3})} \geq \sqrt{E_T \frac{(4 - 2\sqrt{2})\sigma^2}{1 + (3 - 2\sqrt{2})\sigma^2/\sigma_a^2}}$  because the distance of the subsystem #a is greater with  $\mathbf{F}_{r1}$  than  $\mathbf{F}_{octa}$  (the optimal solution is obtained with  $\mathbf{F}_{r1}$  because  $\gamma_a < \gamma_0$ ). In addition, by using the result in ii) we can write the following inequality:  $\sqrt{E_T \frac{(4 - 2\sqrt{2})\sigma^2}{1 + (3 - 2\sqrt{2})\sigma^2/\sigma_a^2}} > \sqrt{E_T \frac{(4 - 2\sqrt{2})\sigma^2}{1 + (3 - 2\sqrt{2})\sigma^2/\sigma_b^2}} = \delta(\sigma_b, \sigma)$ , then (40a) is verified. ■

*Proof of (40b):* we denote subsystem #a the subsystem using  $(\sigma, \sigma_a)$  and subsystem #b the subsystem using  $(\sigma, \sigma_b)$ . Three

cases have to be studied when  $\sigma \geq \sigma_a \geq \sigma_b$ :

i) both subsystems use  $\mathbf{F}_{r1}$

The distances of the subsystems #a and #b are given by:  $\delta(\sigma, \sigma_a) = \delta(\sigma, \sigma_b) = \sigma \sqrt{E_T(1 - 1/\sqrt{3})}$ . Equation (40b) is then verified (equality).

ii) both subsystems use  $\mathbf{F}_{octa}$

The distance of the precoder  $\mathbf{F}_{octa}$  can be expressed as:

$$\delta(\sigma_1, \sigma_2) = \sqrt{E_T \frac{(4 - 2\sqrt{2})\sigma_1^2}{\sigma_1^2/\sigma_2^2 + (3 - 2\sqrt{2})}}$$

For a fixed  $\sigma_1 = \sigma$ , this function is strictly increasing with  $\sigma_2$ . Consequently, we have  $\delta(\sigma, \sigma_a) > \delta(\sigma, \sigma_b)$ .

iii) subsystems #a and #b use  $\mathbf{F}_{octa}$  and  $\mathbf{F}_{r1}$ , respectively

First, note that  $\sigma_a < \sigma_b$  implies  $\gamma_a > \gamma_0 > \gamma_b$ , then from (10)-(12) subsystem #a uses  $\mathbf{F}_{octa}$  and subsystem #b uses  $\mathbf{F}_{r1}$ . The inverse case is then not possible. The distance of the subsystem #a can be lower bounded as:  $\delta(\sigma, \sigma_a) = \sqrt{E_T \frac{(4 - 2\sqrt{2})\sigma^2}{\sigma^2/\sigma_a^2 + (3 - 2\sqrt{2})}} > \sigma \sqrt{E_T(1 - 1/\sqrt{3})}$  because the distance of the subsystem #a is greater with  $\mathbf{F}_{octa}$  than  $\mathbf{F}_{r1}$  (the optimal solution is obtained with  $\mathbf{F}_{octa}$  because  $\gamma_a > \gamma_0$ ). Consequently,  $\delta(\sigma, \sigma_a) > \delta(\sigma, \sigma_b) = \sigma \sqrt{E_T(1 - 1/\sqrt{3})}$ .

*Proof of (40c):* since  $\sigma_a > \sigma_b > \sigma_c > \sigma_d$ , it follows from (40b) and (40a) that  $\delta(\sigma_a, \sigma_b) > \delta(\sigma_a, \sigma_d)$  and  $\delta(\sigma_a, \sigma_d) > \delta(\sigma_c, \sigma_d)$ . ■

Thanks to these three properties, Lemma 1 will be proven in the following by mathematical induction.

## B. The base clause

Let us consider four ordered values  $\sigma_1 > \sigma_2 > \sigma_3 > \sigma_4$ . There are three possible combinations of couples. Table III shows the three cases and compares the minimum distances. By using (40) in Table III, one can conclude that the minimum distance is optimized with the couples  $(\sigma_1, \sigma_4)$  and  $(\sigma_2, \sigma_3)$ .

## C. The induction step

**Hypothesis:** let us consider  $b - 2$  ordered singularvalues such as  $\alpha_1 > \alpha_2 > \dots > \alpha_{b-2}$  ( $b \geq 6$ ). The combination of couples maximizing (19) is:

$$(\alpha_1, \alpha_{b-2}), (\alpha_2, \alpha_{b-3}), \dots, (\alpha_{b/2-1}, \alpha_{b/2}) \quad (41)$$

Let us now consider  $b$  singularvalues such as  $\sigma_1 > \sigma_2 > \dots > \sigma_{b-1} > \sigma_b$ . The number of cases to study is equal to  $\prod_{i=1}^{b/2} (b - 2i + 1) = (b - 1)(b - 3) \dots \times 3 \times 1$ , but it can be reduced as follows. Indeed, let us consider all the couples including  $\sigma_1$ . There are still  $b - 2$  values to be associated, but the starting hypothesis gives the combination that maximizes the minimum distance. It ensues that the number of cases is now  $b - 1$ . Without loss of generality and for the sake of clarity, Table IV shows the optimized solution for  $b = 8$ . For the cases 1 to  $b - 2 = 6$ , the couple achieving the minimum distance remains undetermined (columns 2 to  $b/2 = 4$  in Table IV), but the couple including  $\sigma_1$  never gives the minimum distance and can be discarded thanks to (40). For example, in the case

TABLE III

THE THREE POSSIBLE COMBINATIONS OF COUPLES FOR  $b = 4$  ( $\sigma_1 > \sigma_2 > \sigma_3 > \sigma_4$ ) WITH THEIR ASSOCIATED MINIMUM DISTANCES

combination	Couples	Properties which determines $d_{\min}$ of the combination	Minimum distance	$d_{\min}$ comparison between cases
Case 1	$(\sigma_1, \sigma_2)$ $(\sigma_3, \sigma_4)$	$\delta(\sigma_1, \sigma_2) \geq \delta(\sigma_3, \sigma_4)$	$\delta(\sigma_3, \sigma_4)$	—
Case 2	$(\sigma_1, \sigma_3)$ $(\sigma_2, \sigma_4)$	$\delta(\sigma_1, \sigma_3) \geq \delta(\sigma_2, \sigma_4)$	$\delta(\sigma_2, \sigma_4)$	$\delta(\sigma_2, \sigma_4) \geq \delta(\sigma_3, \sigma_4)$
Case 3	$(\sigma_1, \sigma_4)$ $(\sigma_2, \sigma_3)$	—	UNDETERMINED	$\delta(\sigma_1, \sigma_4) \geq \delta(\sigma_2, \sigma_4)$ $\delta(\sigma_2, \sigma_3) \geq \delta(\sigma_2, \sigma_4)$

6,  $\delta(\sigma_1, \sigma_7) > \delta(\sigma_2, \sigma_8)$  then the association  $(\sigma_1, \sigma_7)$  doesn't give the minimum distance and is discarded.

Otherwise, by using properties (40), the largest distance of the column  $i$  in Table IV is obtained with the association  $(\sigma_i, \sigma_{b-i})$ . Thus, the minimum distance is maximized in the case  $b - 1 = 7$  and Lemma 1 is proven.

One should note that some different combinations of couple should give the same optimized minimum distance. For example, if  $\delta(\sigma_3, \sigma_6)$  is the minimum distance in the case 6 than the two following associations give the same minimum distance:  $\{(\sigma_1, \sigma_8)(\sigma_2, \sigma_7)(\sigma_3, \sigma_6)(\sigma_4, \sigma_5)\}$  and  $\{(\sigma_1, \sigma_7)(\sigma_2, \sigma_8)(\sigma_3, \sigma_6)(\sigma_4, \sigma_5)\}$ .

APPENDIX II  
 PROOF OF LEMMA 2

A. Lower bound

The E- $d_{\min}$  optimized minimum distance is given by (19) and (25), and is lower bounded as:

$$E_T \frac{2}{b} \min_i \tilde{d}_i^2 \leq d_{\min}^2 = E_T \left( \sum_{k=1}^{b/2} \frac{1}{\tilde{d}_k^2} \right)^{-1} \quad (42)$$

We recall that  $\tilde{d}_i$  is given by (26). From (13), let us derive the relation:

$$\xi \lambda_i \leq \tilde{d}_i^2 \leq \lambda_i \quad \text{with } i = 1, \dots, b/2 \quad (43)$$

where  $\xi = 1 - \frac{1}{\sqrt{3}}$ . The eigenvalues  $\lambda_i$  are ordered as  $\lambda_1 > \lambda_2 > \dots > \lambda_{b/2}$  and consequently:

$$\xi \lambda_{b/2} \leq \tilde{d}_i^2 \quad \forall i = 1, \dots, b/2 \quad (44)$$

By using (43), we obtain:

$$\xi \lambda_{b/2} \leq \min_i \tilde{d}_i^2. \quad (45)$$

At the end, it leads to the lower bound:

$$E_T \frac{2}{b} \xi \lambda_{b/2} \leq d_{\min}^2. \quad (46)$$

B. Upper bound

One can write:

$$\sum_{k=1}^{b/2} \frac{1}{\tilde{d}_k^2} = \frac{1}{\tilde{d}_{b/2}^2} \left( 1 + \sum_{k=1}^{b/2-1} \frac{\tilde{d}_{b/2}^2}{\tilde{d}_k^2} \right) \geq \frac{1}{\tilde{d}_{b/2}^2}$$

and deduce the upper bound thanks to (43):

$$d_{\min}^2 \leq \tilde{d}_{b/2}^2 \leq E_T \lambda_{b/2}. \quad (47)$$

REFERENCES

- [1] G. Foschini, "Layered space-time architecture for wireless communication in a fading environment when using multi-element antennas," *Bell Labs. Tech. J.*, pp. 41–59, Autumn 1996.
- [2] I. Telatar, "Capacity of multi-antenna Gaussian channels," *Eur. Trans. Telecomm. ETT*, vol. 10, no. 6, pp. 585–595, Nov. 1999.
- [3] S. M. Alamouti, "A simple diversity technique for wireless communications," *IEEE J. Select. Areas Commun.*, vol. 16, pp. 1451–1458, Oct. 1998.
- [4] V. Tarokh, N. Seshadri, and A. R. Calderbank, "Space-time codes for high data rate wireless communication: Performance criterion and code construction," *IEEE Trans. Inform. Theory*, vol. 44, pp. 744–765, Mar. 1998.
- [5] V. Tarokh, H. Jafarkhani, and A. R. Calderbank, "Space-time codes from orthogonal designs," *IEEE Trans. Inform. Theory*, vol. 45, no. 5, pp. 1456–1467, Jul. 1999.

TABLE IV

GENERALIZATION TO  $b = 8$  SINGULARVALUES ASSUMING HYPOTHESIS FOR  $b - 2 = 6$  SINGULARVALUES

Combinations (assuming hypothesis)					Minimum distance may be achieved by:			
hypothesis					column 1	column 2	column 3	column 4
case 1	$(\sigma_1, \sigma_2)$	$(\sigma_3, \sigma_8)$	$(\sigma_4, \sigma_7)$	$(\sigma_5, \sigma_6)$		$(\sigma_3, \sigma_8)$	$(\sigma_4, \sigma_7)$	$(\sigma_5, \sigma_6)$
case 2	$(\sigma_1, \sigma_3)$	$(\sigma_2, \sigma_8)$	$(\sigma_4, \sigma_7)$	$(\sigma_5, \sigma_6)$		$(\sigma_2, \sigma_8)$	$(\sigma_4, \sigma_7)$	$(\sigma_5, \sigma_6)$
case 3	$(\sigma_1, \sigma_4)$	$(\sigma_2, \sigma_8)$	$(\sigma_3, \sigma_7)$	$(\sigma_5, \sigma_6)$		$(\sigma_2, \sigma_8)$	$(\sigma_3, \sigma_7)$	$(\sigma_5, \sigma_6)$
case 4	$(\sigma_1, \sigma_5)$	$(\sigma_2, \sigma_8)$	$(\sigma_3, \sigma_7)$	$(\sigma_4, \sigma_6)$		$(\sigma_2, \sigma_8)$	$(\sigma_3, \sigma_7)$	$(\sigma_4, \sigma_6)$
case 5	$(\sigma_1, \sigma_6)$	$(\sigma_2, \sigma_8)$	$(\sigma_3, \sigma_7)$	$(\sigma_4, \sigma_5)$		$(\sigma_2, \sigma_8)$	$(\sigma_3, \sigma_7)$	$(\sigma_4, \sigma_5)$
case 6	$(\sigma_1, \sigma_7)$	$(\sigma_2, \sigma_8)$	$(\sigma_3, \sigma_6)$	$(\sigma_4, \sigma_5)$		$(\sigma_2, \sigma_8)$	$(\sigma_3, \sigma_6)$	$(\sigma_4, \sigma_5)$
case 7	$(\sigma_1, \sigma_8)$	$(\sigma_2, \sigma_7)$	$(\sigma_3, \sigma_6)$	$(\sigma_4, \sigma_5)$	$(\sigma_1, \sigma_8)$	$(\sigma_2, \sigma_7)$	$(\sigma_3, \sigma_6)$	$(\sigma_4, \sigma_5)$
largest distance for each column $\implies$					$\delta(\sigma_1, \sigma_8)$	$\delta(\sigma_2, \sigma_7)$	$\delta(\sigma_3, \sigma_6)$	$\delta(\sigma_4, \sigma_5)$

- [6] D. P. Palomar, J. M. Cioffi, and M. A. Lagunas, "Joint Tx-Rx beamforming design for multicarrier MIMO channels: A unified framework for convex optimization," *IEEE Trans. Signal Processing*, vol. 51, no. 9, pp. 2381–2401, Sept. 2003.
- [7] T. K. Lo, "Maximum ratio transmission," *IEEE Trans. Commun.*, vol. 47, no. 10, pp. 1458–1461, Oct. 1999.
- [8] P. Stoica and G. Ganesan, "Maximum-SNR spatial-temporal formatting designs for MIMO channels," *IEEE Trans. Signal Processing*, vol. 50, no. 12, pp. 3036–3042, Dec. 2002.
- [9] H. Sampath, P. Stoica, and A. Paulraj, "Generalized linear precoder and decoder design for MIMO channels using the weighted MMSE criterion," *IEEE Trans. Commun.*, vol. 49, no. 12, pp. 2198–2206, Dec. 2001.
- [10] A. Scaglione, P. Stoica, S. Barbarossa, G. Giannakis, and H. Sampath, "Optimal designs for space-time linear precoders and decoders," *IEEE Trans. Signal Processing*, vol. 50, no. 5, pp. 1051–1064, May 2002.
- [11] P. Rostaing, O. Berder, G. Burel, and L. Collin, "Minimum BER diagonal precoder for MIMO digital transmissions," *Signal Processing*, vol. 82, no. 10, pp. 1477–1480, Oct. 2002.
- [12] D. P. Palomar and Y. Jiang, *MIMO Transceiver Design via Majorization Theory*. Foundations and Trends in Communications and Information Theory, Now Publishers, 2006, vol. 3, no. 4-5.
- [13] L. Collin, O. Berder, P. Rostaing, and G. Burel, "Optimal minimum distance-based precoder for MIMO spatial multiplexing systems," *IEEE Trans. Signal Processing*, vol. 52, no. 3, pp. 617–627, Mar. 2004.
- [14] B. Vrigneau, J. Letessier, P. Rostaing, and L. Collin, "Statistical comparison between max- $d_{\min}$ , max-SNR and MMSE precoders," *the 40th IEEE Asilomar Conference on Signals, Systems and Computers*, 2006.
- [15] B. Vrigneau, J. Letessier, P. Rostaing, L. Collin, and G. Burel, "max- $d_{\min}$  precoder performances in a polarity diversity MIMO channel," *the 40th Asilomar Conference on Signals, Systems and Computers*, 2006.
- [16] L. Zheng and D. Tse, "Diversity and multiplexing: a fundamental tradeoff in multiple-antenna channels," *IEEE Trans. Inform. Theory*, vol. 49, no. 5, pp. 1073–1096, May 2003.
- [17] L. G. Ordóñez, D. P. Palomar, A. Pages-Zamora, and X. R. Fonollosa, "High-SNR analytical performance of spatial multiplexing MIMO systems with CSI," *IEEE Trans. Signal Processing*, vol. 55, no. 11, pp. 5447–5463, Nov. 2007.
- [18] E. Sengul, E. Akay, and E. Ayanoglu, "Diversity analysis of single and multiple beamforming," *IEEE Trans. Commun.*, vol. 54, no. 6, pp. 990–993, June 2006.
- [19] A. Paulraj, R. Nabar, and D. Gore, *Introduction to space-time wireless communications*. Cambridge University Press, 2003.
- [20] X. Zhu and R. Murch, "Performance analysis of maximum likelihood detection in a MIMO antenna system," *IEEE Trans. Commun.*, vol. 50, pp. 187–191, Feb. 2002.
- [21] IEEE P802.11 Wireless LANs, "Joint proposal: High throughput extension to the 802.11 standard: Phy., Tech. Rep. IEEE 802.11-05/1102r4, Jan. 2006.
- [22] C. Shen and M. P. Fitz, "MIMO-OFDM beamforming for improved channel estimation," in *GLOBECOM'06*.
- [23] J. Proakis, *Digital Communications*, 4th ed., 2000.
- [24] ETSI EP BRAN#9, *Criteria for Comparison*, 30701F-WG3 PHY subgroup, may 1998.



**Jonathan Letessier** was born at Fougères, France, in 1978. In 2001 and 2002, he successively received a B.Sc degree and a M.Sc one in Telecommunication and Communication Processing before successfully defending, in 2005, his Ph.D. in Electrical engineering at the University of Brest (France). Since 2005 he has been Assistant Professor and works as member of the Laboratory for Electronics and Telecommunication Systems (LEST-UMR CNRS 6165). His research interests are focused on MIMO systems.



**Philippe Rostaing** received the Ph.D degree in electrical engineering from the University of Nice-Sophia Antipolis, France, in 1997. From 1997 to 2000, he was Assistant Professor at the French Naval Academy, Lanveoc, France. Since 2000, he has been Assistant Professor of Digital Communications and Signal Processing at the University of Brest. He is a member of the Laboratory LEST - UMR CNRS 6165. His present research interests are in signal processing for digital communications with emphasis on MIMO systems.



**Ludovic Collin** received the Ph.D. degree in electrical engineering from the University of Bretagne Occidentale, Brest, France, in 2002. From 1989 to 1999 he was with ORCA Instrumentation, Brest, where he developed oceanographical instrumentation and acoustic modems. From December 1999 to September 2002, he was a Research and Teaching Assistant at French Naval Academy, Lanveoc, France. Since September 2002, he has been Assistant Professor at the Institut of Technology of Lannion, and at the ENSIETA, Brest. He is a member of the Laboratory for Electronics and Telecommunication Systems (LEST-UMR CNRS 6165) and his research interests are in MIMO systems and interception of communications.



**Baptiste Vrigneau** was born at Lannion (France) in 1979. He received the M.Sc degrees from École Normale Supérieure de Cachan, France, in 2001, and the Ph.D. degree from University of Brest, France, in 2006. From September 2003 to August 2007, he was a member of the Laboratory for Electronics and Telecommunication System (LEST-UMR CNRS 6165), France. Since, September 2007, he has been Assistant Professeur at the Institute of Technology of Lannion and works with CAIRN (former R2D2) IRISA project, France. His research interests are

focused on MIMO systems, sensors network, and Computing Architectures.



**Gilles Burel** was born in 1964. He received the M.Sc. degree from École Supérieure d'Electricité, Gif Sur Yvette, France, in 1988 and the Ph.D. degree from University of Brest, France, 1991. From 1988 to 1997 he was a member of the technical staff of Thomson CSF, then Thomson Multimedia, Rennes, France, where he worked on image processing and pattern recognition applications as project manager. Since 1997, he has been Professor of Digital Communications, Image and Signal Processing at the University of Brest. He is a member of the Laboratory for Electronics and Telecommunication Systems (LEST-UMR CNRS 6165) and, within this laboratory, he is Director of the Signal Processing Team. He is the author of 19 patents, one book and more than one hundred scientific papers. His present research interests are in signal processing for digital communications with emphasis on MIMO systems, interception of communications and chaotic transmissions.

He is the author of 19 patents, one book and more than one hundred scientific papers. His present research interests are in signal processing for digital communications with emphasis on MIMO systems, interception of communications and chaotic transmissions.